American Mineralogist, Volume 94, pages 1672–1678, 2009

The hydrothermal conversion of kaolinite to kalsilite: Influence of time, temperature, and pH

Ana Isabel Becerro,[1,*] Alberto Escudero,[2] and Marco Mantovani[1]

[1]Instituto de Ciencia de Materiales de Sevilla-Departamento de Química Inorgánica (CSIC-US), 41092 Sevilla, Spain
[2]Bayerisches Geoinstitut, Universität Bayreuth, 95440 Bayreuth, Germany

Abstract

Kalsilite (the low-temperature form of $KAlSiO_4$) is used as the precursor of leucite, an important component in porcelain-fused-to-metal and ceramic-restoration systems, and it has also been proposed as a high-thermal expansion ceramic for bonding to metals. The present study reports the hydrothermal synthesis and characterization of pure kalsilite from kaolinite in subcritical conditions, as well as the characterization of the intermediate products by means of XRD, ^{29}Si and ^{27}Al MAS NMR, IR, SEM, and TEM. Effects of time, temperature, and pH on the reaction products are analyzed. The experimental data indicate that pure kalsilite is obtained after hydrothermal treatment of kaolinite at 300 °C for 12 h in 0.5 *M* KOH solution. Longer reaction times increase the crystallinity of the structure, whereas lower reaction times give rise to the metastable ABW-type $KAlSiO_4$ polymorph. Lower temperatures are not sufficient to produce kalsilite, but zeolite W is obtained instead as the unique reaction product. Finally, the pH of the aqueous solution in contact with kaolinite is an important parameter for the synthesis of kalsilite, which must be ≥13.70.

Keywords: Kalsilite, kaolinite, hydrothermal synthesis, MAS NMR, XRD

Introduction

$KAlSiO_4$ is a feldspathoid that, like zeolites, has a framework structure of linked $(Si,Al)O_4$ tetrahedra. $KAlSiO_4$ exists in several polymorphic forms (Cellai et al. 1997): (1) low kalsilite ($P6_3$, known simply as kalsilite) (Perrotta and Smith 1965), which is a stuffed tridymite derivative occurring mainly in K-rich silica undersaturated volcanic rocks, and (2) its high-temperature form known as high kalsilite (space group $P6_3mc$) (Kawahara et al. 1986). Another high-temperature polymorph is the orthorhombic $KAlSiO_4$-O1, which has an $AlSiO_4$ framework that is a topological variant of tridymite with space group $P12_11$ (Gregorkiewitz et al. 2008) and undergoes a mineral transformation into $KAlSiO_4$-O2 at >1450 °C (Cook et al. 1977). Another phase named kaliophilite has been described with a unit cell that is a multiple of the kalsilite cell (space group $P6_322$; Cellai et al. 1992). Finally, a metastable polymorph of $KAlSiO_4$ was prepared by Minor et al. (1978) by K^+ exchange of orthorhombic $RbAlSiO_4$; it shows orthorhombic symmetry (*Ccmm*) and retains the ABW zeolite compatible unit cell of $RbAlSiO_4$, showing doubling of the *b*- and *c*-axes relative to the normal ABW-type cell; this polymorph transforms into normal "low kalsilite" at 1100 °C (Norby and Fjellvåg 1992).

Kalsilite has been studied as the precursor of leucite, an important component in porcelain-fused-to-metal (PFM) and ceramic dental-restoration systems (Zhang et al. 2007). Kalsilite has also been proposed as a high-thermal expansion ceramic for bonding to metals (Bogdanoviciene et al. 2008). Very recently, nano-kalsilite has been demonstrated to show an excellent and highly improved oxidation activity toward carbon in diesel soot combustion (Kimura et al. 2008). All of these uses require the production of single-phase kalsilite.

Reviews of related literature show very different methods for the synthesis of kalsilite: (1) cation exchange from nepheline (Dollase and Freeborn 1977; Stebbins et al. 1986; Sobrados and Gregorkiewitz 1993); (2) solid-state synthesis from oxides or zeolite (Smith and Tuttle 1957; Dimitrijevic and Dondur 1995; Heller-Kallai and Lapides 2003; Kosanović et al. 1997); (3) sol-gel methods using TEOS or SiO_2 as a Si source (Hamilton and Henderson 1968; Bogdanoviciene et al. 2007); (4) crystallization from molten salts (Sobrados and Gregorkiewitz 1993); and (5) hydrothermal methods from muscovite or oxides as substrates (Barrer et al. 1951, 1956, 1968, 1972; Kopp et al. 1961; Andou and Kawahara 1984). Many of these methods give rise to secondary products or to poorly ordered kalsilite.

Compared with other synthesis methods, the hydrothermal method is economical and convenient to prepare pure materials with fine particle size at low temperature. However, the hydrothermal methods referenced above to obtain kalsilite, use high pressures (1000 bars), relatively high temperatures (up to 600 °C), and long reaction times (15 days), with a consequent increase in the production cost. The present study reports the hydrothermal transformation of kaolinite, a natural and readily available precursor, into kalsilite at subcritical conditions with a full characterization of the intermediate and final reaction products by means of X-ray diffraction (XRD), Fourier transform infrared spectroscopy (FTIR), magic angle spinning nuclear magnetic resonance spectroscopy (MAS NMR), transmission electron microscopy (TEM), and energy dispersive X-ray spectrometry (EDX). Effects of time, temperature, and pH on the synthesis products are analyzed.

* E-mail: anieto@icmse.csic.es

0003-004X/09/1112–1672$05.00/DOI: 10.2138/am.2009.3284

Experimental methods

Hydrothermal reactions

Kaolinite KGa-1b, chemical formula $(Si_{3.83}Al_{0.17})^{IV}(Al_{3.86}Fe_{0.02}Ti_{0.11})^{VI}(Ca,Na,K,Mg)_{0.05}O_{10}(OH)_8$, was supplied by the Source Clay Minerals Repository, University of Missouri (Columbia). Three hundred milligrams of KGa-1b kaolinite were mixed with 50 mL of 0.5 *M* KOH solution in a stainless steel hydrothermal reactor and heated at 300 °C at 10 °C/min for 1, 3, 6, 9, 12, 24, 48, and 120 h. The pressure inside the reactor was that corresponding approximately to the vapor pressure of water at that temperature (8.58 MPa). After cooling at room temperature, the products were filtered and washed repeatedly with distilled water and dried at 60 °C in air. To analyze the effect of pH, additional experiments were carried out at 300 °C with the same amount of kaolinite and the following aqueous solutions: 50 mL KOH 0.15 *M*, 50 mL KOH 0.33 *M*, and 50 mL (KOH 0.33 *M* + NaOH 0.17 *M*), for 24 h. Hydrothermal experiments at 200 °C in KOH 0.5 *M* were conducted as well to test the effect of temperature on the nature of the reaction product.

Characterization techniques

Routine powder XRD patterns were collected using a Siemens D-501 diffractometer with Ni-filtered Cu*K*α radiation, in the 2θ range 5 to 60°, steps of 0.05°, and counting time of 5 s per step. In addition, the product obtained after reaction of kaolinite with 0.5 *M* KOH solution at 300 °C for 120 h was analyzed by XRD in the 2θ range 5 to 120°, steps of 0.02°, and counting time of 10 s to carry out a Rietveld refinement with the TOPAS software (Cheary and Coelho 1992). Refined parameters were: background coefficients, lattice constants, strains, crystal size, atomic coordinates, and isotropic temperature factors.

^{29}Si MAS NMR spectroscopy measurements were carried out in a Bruker DRX400 (9.39 T) spectrometer equipped with a multinuclear probe, using 4 mm zirconia rotors spinning at 10 kHz. A single pulse sequence was used, with a pulse length of 2.5 μs (π/2 pulse length = 7.5 μs), an observation frequency for ^{29}Si of 79.49 MHz, and an optimized delay time of 100 s. The chemical shifts are reported in parts per million from tetramethylsilane (TMS). ^{27}Al MAS NMR spectra were recorded at 104.26 MHz with a pulse length of 1.1 μs (π/2 pulse length = 11 μs) and a delay time of 0.5 s. The chemical shifts are reported in parts per million from a 0.1 *M* $AlCl_3$ solution. The experimental ^{29}Si NMR spectra of the starting materials and the reaction products have been fitted using a modified version of the Bruker Winfit program, which handles the finite spinning speed in MAS experiments (Massiot et al. 2002).

FTIR spectroscopy was carried out using a Nicolet 510 FTIR instrument equipped with a DTGS detector. Spectra were recorded in the 1400–400 cm^{-1} range with a resolution of 2 cm^{-1}. The measurements were made using dried KBr pellets, which were prepared by mixing and pressing 1 mg of sample with 100 mg KBr. Scanning electron microscopy was carried out in a JEOL JSM 5400 microscope equipped with a LINK Pentafet probe and ATW windows for EDX analysis. Finally, TEM (Philips 200 CM) were used to examine the morphology of the samples while the chemical composition of individual particles was studied by EDX analysis using a Philips DX4 instrument attached to the microscope. The samples were dispersed in ethanol by sonication and dropped on a conventional carbon-coated copper grid.

Results and discussion

Hydrothermal transformation of kaolinite at 300 °C with increasing reaction time

Figure 1 shows the XRD patterns of the products obtained after hydrothermal reaction of kaolinite in 0.5 *M* KOH solution at increasing time. After 1 h reaction, the pattern shows a high background of amorphous material with several reflections emerging from it that indicate an incipient crystallization of the metastable orthorhombic polymorph of $KAlSiO_4$ with an ABW-type compatible unit cell (Minor et al. 1978; Norby and Fjellvåg 1992) (space group *Ccmm*; PDF 31-965). The rest of the reflections belong to zeolite F (PDF 38-216), although the one expected at 31.9 °2θ corresponding to this phase is missing in the pattern. Low-intensity reflections of anatase (PDF 21-1272) can also be observed. Zeolite F disappears after 6 h

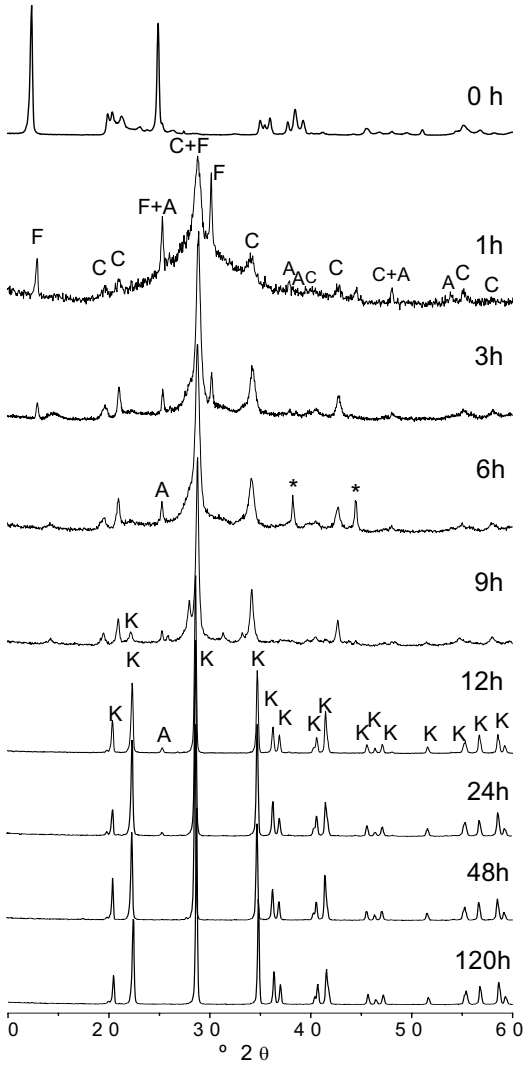

Figure 1. XRD patterns of starting kaolinite and products obtained after hydrothermal treatment of kaolinite in 0.5 *M* KOH solution at 300 °C for 1, 3, 6, 9, 12, 24, 48, and 120 h. F = Zeolite F, C = ABW-type $KAlSiO_4$, A = Anatase, K = Kalsilite. * = Al from the X-ray sample holder.

treatment, whereas the degree of crystallinity of the ABW-type $KAlSiO_4$ polymorph increases with time, reaching its maximum after 9 h of reaction, as inferred from the resolution of the reflections. A low-intensity reflection at ~22.3 °2θ in the pattern of the latter sample suggests the formation of some kalsilite crystals ($KAlSiO_4$, space group $P6_3$: PDF 85-1413). A detailed examination of the XRD pattern of the sample treated for 6 h reveals the presence of a broad contribution at the same 2θ value, suggesting that nucleation of kalsilite has started by that time. The ABW-type $KAlSiO_4$ crystals show a needle-like appearance, as shown in Figure 2a for the sample treated for 3 h. When the hydrothermal reaction goes on for 12 h, metastable ABW-type $KAlSiO_4$ transforms completely into kalsilite, forming hexagonal platelets with clean edges (Fig. 2b). All of the XRD patterns of the products obtained after 12, 24, 48, and 120 h (Fig. 1) show reflections characteristic of kalsilite, plus very low-intensity

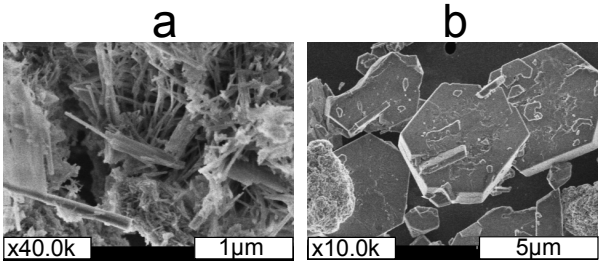

FIGURE 2. SEM micrographs of (**a**) needle-like particles of ABW-type $KAlSiO_4$ obtained after 3 h treatment of kaolinite in 0.5 *M* KOH solution at 300 °C and (**b**) hexagonal particles of kalsilite obtained after 12 h treatment of kaolinite in 0.5 *M* KOH solution at 300 °C.

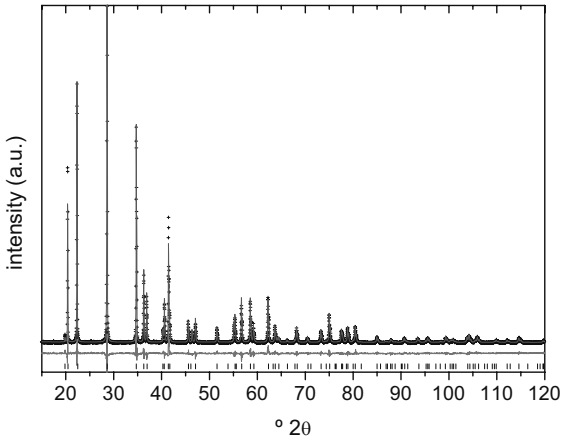

FIGURE 3. Experimental (crosses) and fitted (solid line) X-ray diffraction patterns of the product obtained after hydrothermal reaction of kaolinite in 0.5 *M* KOH solution for 120 h. The difference curve is also shown.

reflections of anatase, which decrease with increasing reaction time until complete disappearance after 48 h.

The XRD pattern of the sample obtained after 120 h of hydrothermal reaction has been analyzed using the Rietveld method with the TOPAS software (Fig. 3). The starting parameters were those of Andou and Kawahara (1984), who used a synthetic kalsilite sample to establish the crystal structure. All the reflections could be indexed on the basis of a hexagonal unit cell with space group $P6_3$. Unit-cell parameters were $a = 5.1666(1)$ and $c = 8.7123(1)$ Å, slightly higher than those of Andou and Kawahara (1984) [$a = 5.151(5)$, $c = 8.690(8)$ Å], and more similar to those given by Perrotta and Smith (1965) [$a = 5.161(4)$, $c = 8.693(5)$ Å], who used a natural kalsilite sample. Atomic parameters are given in Table 1.

^{29}Si and ^{27}Al MAS NMR spectra (Figs. 4a and 4b, respectively) of the reaction products of kaolinite in 0.5 *M* KOH solution after 6, 9, 12, 24, 48, and 120 h have been recorded to obtain information about the evolution of the local structure around the nuclei. The ^{29}Si MAS NMR spectra of the samples treated for 6 and 9 h show a broad band that can be decomposed into three different resonances. Values obtained from the deconvolution of both spectra have been included in Table 2. The chemical shift of the resonance at ~ –86 ppm is in the range expected for $Q^4(4Al)$ environments and must correspond to the Si nuclei in ABW-type $KAlSiO_4$. The signal shows a high full-width at half maximum (FWHM) value suggesting non-equivalent Si sites in the asymmetric unit, which is consistent with the doubling of the *b*- and *c*-axes of the ABW-type $KAlSiO_4$ unit cell relative to the normal ABW-type cell (Norby and Fjellvåg 1992). This fact was already noticed by Norby and Fjellvåg (1992) but, to the best of our knowledge, they never published ^{29}Si NMR chemical shifts or FWHM values. The area under the curve of this resonance does not change much on passing from 6 to 9 h treatment, whereas the FWHM value decreases slightly, indicating an increase in the order around the Si nuclei, in good agreement with the XRD observations. The resonance at –89 ppm obtained in the deconvolution of these spectra corresponds to the unique Si type of environment in the kalsilite structure, $Q^4(4Al)$. The resonance shows a pronounced decrease in the FWHM as well as an increase in the area under the curve with increasing reaction time from 6 to 9 h, in agreement with the XRD data that indicated an increase in both the proportion and the crystallinity of kalsilite with increasing reaction time. Finally, a broad resonance centered at ~ –93 ppm is observed in both spectra, which cannot be assigned to rests of the starting kaolinite due to the absence of any resonance of octahedral Al in the corresponding ^{27}Al MAS NMR spectra. This broad band is possibly due to the presence of amorphous features that are not detected in the XRD patterns and whose proportion decreases with increasing reaction time. Similar observations were made in Gregorkiewitz et al. (2008) after the ceramic synthesis of the "orthorhombic" $KAlSiO_4$-O1 polymorph.

The ^{29}Si MAS NMR spectra of the samples treated for 12, 24, 48, and 120 h show a unique resonance at –89.1 ppm corresponding to the unique Si type of environment in the kalsilite structure, $Q^4(4Al)$. Two ^{29}Si MAS NMR studies on kalsilite have been found in the literature (Stebbins et al. 1986; Hovis et al. 1992); they show the main $Q^4(4Al)$ resonance, although both of them exhibit an additional peak attributed to $Q^4(3Al)$ due to a silica content in excess of the ideal 1:1 Si/Al ratio (the samples were prepared from a natural nepheline by ion exchange in molten KBr for 3 days at 1033 K). The presence of a single and narrow ^{29}Si resonance observed here in Figure 4a is consistent with the ideal 1:1 Si/Al ratio and with the Al avoidance principle, resulting in complete Si-Al order in a single-phase kalsilite sample.

The ^{27}Al MAS NMR spectra of the samples treated for 6 and

TABLE 1. Atomic parameters of hydrothermal kalsilite obtained from Rietveld refinement; space group $P6_3$

Atom	Site	Oxidation state	*x*	*y*	*Z*	SOF	B_{eq}
O1	6*c*	–2	0.6119(13)	0.0081(26)	0.9839(9)	1	1.27(8)
O2	6*c*	–2	0.3500(10)	0.7036(80)	0.2583(25)	0.3333	1.44(40)
Si	2*b*	+4	0.33333	0.66667	0.4356(10)	1	0.52(11)
Al	2*b*	+3	0.33333	0.66667	0.0508(11)	1	1.67(16)
K	2*a*	+1	0.00000	0.00000	0.25000	1	1.51(5)

Notes: $a = 5.1666(1)$ Å, $c = 8.7123(1)$ Å. GOF = 1.30; $R_p = 9.54$; $R_{wp} = 12.24$; $R_{Bragg} = 4.998$.

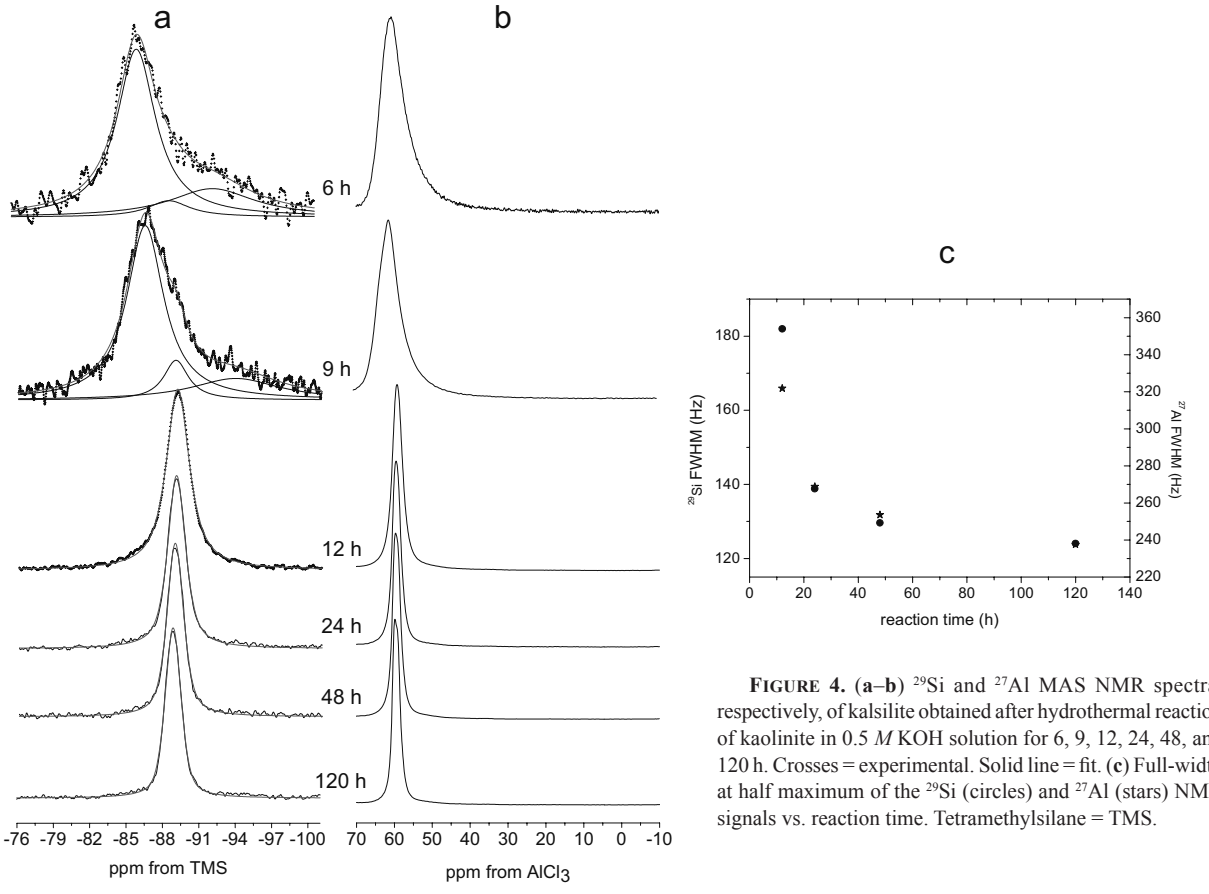

FIGURE 4. (**a**–**b**) ^{29}Si and ^{27}Al MAS NMR spectra, respectively, of kalsilite obtained after hydrothermal reaction of kaolinite in 0.5 *M* KOH solution for 6, 9, 12, 24, 48, and 120 h. Crosses = experimental. Solid line = fit. (**c**) Full-width at half maximum of the ^{29}Si (circles) and ^{27}Al (stars) NMR signals vs. reaction time. Tetramethylsilane = TMS.

9 h (Fig. 4b) show a unique signal centered at 60.8 ppm, which falls in the frequency range of tetrahedral Al, and must contain the contribution of the Al nuclei in both the ABW-type $KAlSiO_4$ and in kalsilite. Increasing reaction time to 12 h and longer, gave rise to ^{27}Al MAS NMR spectra consisting of a unique and symmetric signal centered at 59.3 ppm, consistent with the $q^4(4Si)$ environments in a fully ordered kalsilite structure.

The ^{29}Si and ^{27}Al MAS NMR spectra of the samples treated for 12 h and longer show an exponential decay in the FWHM values (Fig. 4c) with increasing reaction time, indicating an increase in the local order around the Si and Al nuclei of the kalsilite phase with increasing reaction time.

The IR spectra of the samples (Fig. 5) can be clearly divided into two groups: (1) those corresponding to the products of 1, 3, 6, and 9 h reaction; and (2) those of 12, 24, 48, and 120 h reaction. The first group of spectra must correspond to the lattice vibrations of ABW-type $KAlSiO_4$. Two additional bands at ~3440 and 1637 cm^{-1} (not shown) correspond to weak hydrogen bonds of OH groups. The spectrum of the sample reacted for 1 h displays ill-defined bands, possibly due to the low crystallinity of the phase (see XRD pattern in Fig. 1), whereas the rest exhibit very well-defined peaks, in agreement with the XRD data. No IR data of this phase have been found in the literature, but the spectrum is very similar to that of $LiAlSiO_4 \cdot H_2O$ reported by Norby et al. (1986), who commented only on the bands corresponding to the OH groups. By analogy with the IR spectra of other aluminosilicates (Dowty 1987), we can assign the peaks in the range 1200–900 cm^{-1} to T-O (T = Si,Al) asymmetric stretching modes, whereas the 800–400 cm^{-1} region contains the T-O (T = Si,Al) bending modes.

The second group of spectra contains the vibrations of kalsilite molecules; the absorption bands at 460, 478, 684, 985, and 1037 cm^{-1} are in good agreement with the limited data given by Sahama (1965) and by Carpenter and Cellai (1996) for natural specimens and by Henderson and Taylor (1988) for synthetic kalsilite. No absorption bands were observed between 1300 and 4000 cm^{-1} in this case, indicating a complete dehydration of the kalsilite phase. Sahama (1965) noted that the IR absorption band lying between 500 and 520 cm^{-1} in nephelines could be used as an indicator of the potassium content. Extrapolation of Sahama's equation for perpotassic nephelines would place this absorption band at 484 cm^{-1} in pure kalsilite. Whereas Henderson and Taylor (1988) only observed an ill-defined shoulder on the 460 cm^{-1} band, all our spectra (Fig. 5) show a clear shoulder at 478 cm^{-1} that must correspond to such a diagnostic peak.

TABLE 2. ^{29}Si MAS NMR parameters obtained from the fitting of the spectra corresponding to the samples treated for 6 and 9 h in 0.5 *M* KOH solution at 300 °C

6 h			9 h		
^{29}Si Chemical shift (ppm)	FWHM (Hz)	Area under the curve (%)	^{29}Si Chemical shift (ppm)	FWHM (Hz)	Area under the curve (%)
–86.31	308	68	–86.45	294	70
–89.00	329	7	–88.99	195	10
–92.59	671	25	–93.92	700	20

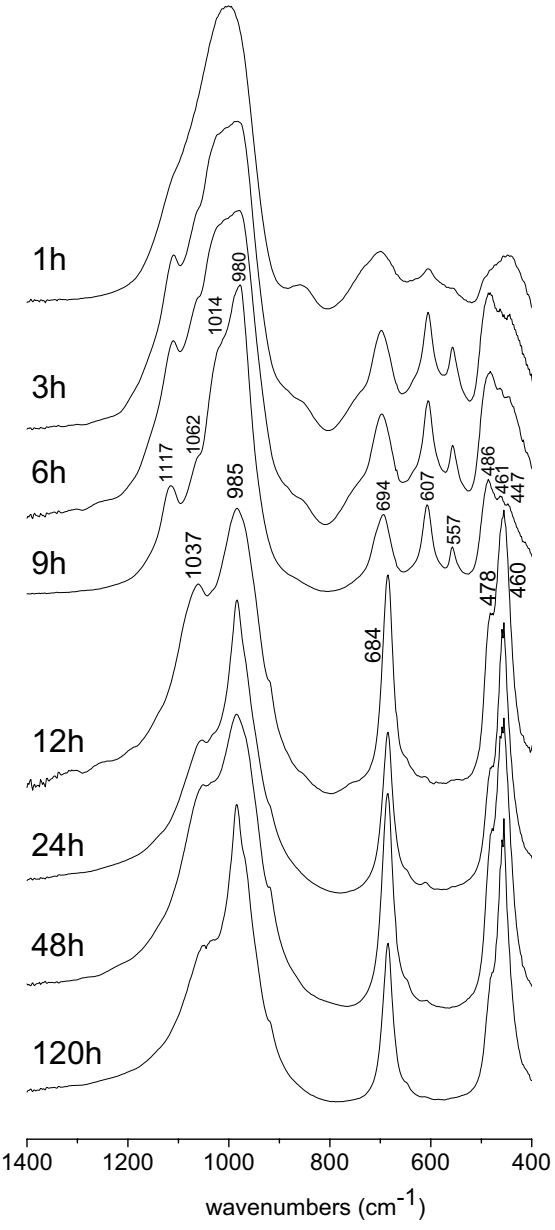

FIGURE 5. IR spectra of the reaction product of kaolinite submitted to hydrothermal reaction in 0.5 *M* KOH solution at 300 °C for 1, 3, 6, 9, 12, 24, 48, and 120 h.

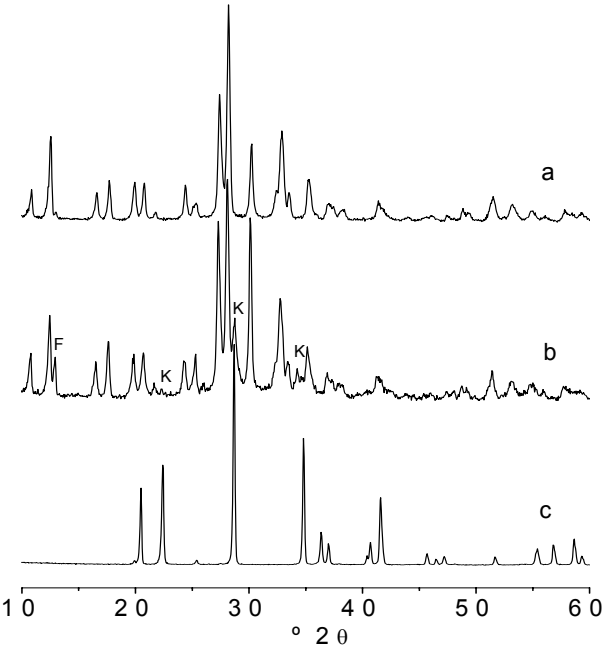

FIGURE 6. XRD pattern of (**a**) zeolite W obtained after hydrothermal reaction of kaolinite in 0.15 *M* KOH solution at 300 °C for 24 h; (**b**) the hydrothermal reaction product of kaolinite in 0.33 *M* KOH solution at 300 °C for 24 h; all reflections correspond to zeolite W except those marked with F = zeolite F and k = kalsilite; and (**c**) kalsilite obtained after hydrothermal reaction of kaolinite in (0.33 *M* KOH + 0.17 *M* NaOH) solution at 300 °C for 24 h.

Influence of pH

Kalsilite formation from kaolinite can be written as:

$$Si_4Al_4O_{10}(OH)_8 + 4\ KOH \rightarrow 4\ KAlSiO_4 + 6\ H_2O.$$

The stoichiometry indicates, therefore, that a minimum of 4 mol KOH are necessary to react with 1 mol kaolinite to obtain 4 mol kalsilite. The synthesis of kalsilite reported above (300 mg kaolinite in 50 mL 0.5 *M* KOH) was reached using a large excess of KOH, that is, around 10 times more KOH than the amount required by the stoichiometry of the reaction. When the concentration of the KOH solution is decreased to 0.15 *M*, zeolite W [a potassium aluminosilicate with chemical formula: $K_{10.32}(Si_{21.7}Al_{10.3}O_{64})(H_2O)_{24.32}$; PDF 86-1110] is formed as the unique phase instead of kalsilite, as observed in Figure 6a. Zeolite W was synthesized by Bieniok et al. (1996) from gels of $Na_2O + K_2O + Al_2O_3 + SiO_2 + H_2O$ in different proportions in autoclave at 150 °C for 24 h. Although Na is present in their reacting medium, the authors concluded that the sodium content in the final product can be neglected and that sodium is not necessary for the crystallization of zeolite W, as also demonstrated in the present experiments. Similar results are observed when the KOH concentration used is 0.33 *M* (Fig. 6b), in which case, zeolite W is formed as the main reaction product accompanied by a small amount of kalsilite and zeolite F. Both concentrations still imply that an excess KOH (ca. 3 and 7 times more than the amount required by the stoichiometry of the reaction, respectively) is present in the reaction media. The formation of a different product is not, therefore, caused by the lack of K in the reaction media but, very likely, by the effect of pH, which increases from pH = 13.18 (0.15 *M* KOH), to pH = 13.52 (0.33 *M* KOH) and to pH = 13.70 (0.5 *M* KOH solution). The results show that increasing alkalinity leads to an increase in the kalsilite content of the reaction product and to a decrease in zeolite W. Similar results were shown by Bieniok et al. (1996) who obtained zeolite W only when the K+Na-Al/Si ratio was between 1.4 and 2.9. At higher alkalinity values, the reaction yielded aluminosilicate phases called L-20 and L-23. To check this hypothesis, the necessary amounts of KOH and NaOH were mixed to make a 50 mL solution of (0.33 *M* KOH + 0.17 *M*

NaOH). This solution has the same KOH concentration as the one described above, but the pH was raised by the presence of NaOH to the same value as that of the 0.5 *M* KOH solution. The result of the synthesis using the KOH/NaOH solution is shown in Figure 6c, where only reflections of kalsilite are observed. The kalsilite particles thus obtained were studied by TEM/EDX, and only K, Si, and Al lines were observed in all the particles analyzed (Fig. 7). The results demonstrate that sodium was not incorporated into the kalsilite structure and that the only role of the NaOH added to the solution was to increase the pH to a value favorable for the formation of kalsilite. A pH difference of only 0.2 pH units is, therefore, decisive for the formation of one or another aluminosilicate.

Influence of temperature

Figure 8 shows the XRD patterns of the products of kaolinite submitted to hydrothermal reaction in 0.5 *M* KOH at 200 °C for 24, 48, and 120 h. After 24 h, the XRD pattern exhibits a high-intensity broad band indicative of the presence of a significant amount of amorphous material. Several narrow reflections emerge from the band, indicating the incipient formation of kalsilite, zeolite W, and anatase. After 48 h, the band of amorphous material disappears and the XRD pattern shows the crystallization of zeolite W and a small reflection of anatase. The same XRD pattern is observed after 120 h reaction. The results indicate that, although kalsilite crystallizes in the first stages of the reaction at 200 °C, very likely as a metastable phase, longer reaction times give rise to the crystallization of zeolite W.

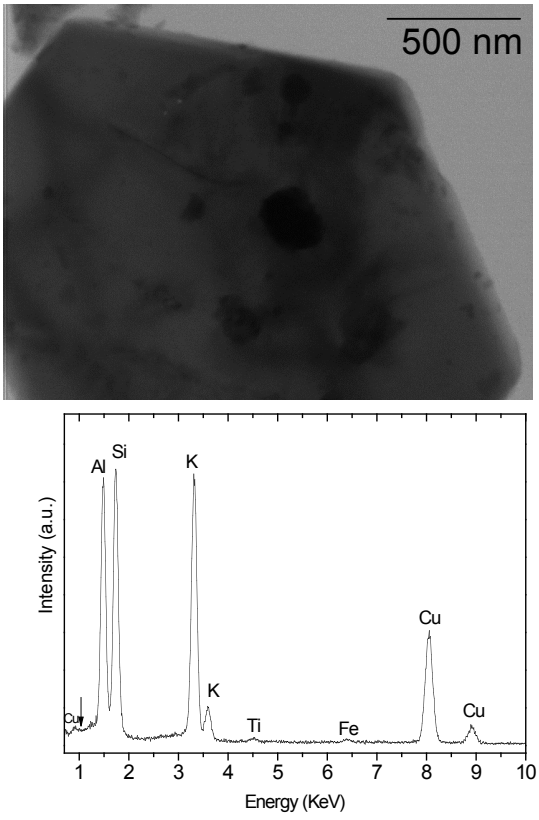

Figure 7. TEM micrograph of an hexagonal kalsilite particle and associated EDX spectrum showing the absence of any lines corresponding to Na. The arrow marks the energy corresponding to the expected position of the Na$K\alpha_1$ line. The product was obtained after hydrothermal reaction of kaolinite in (0.33 *M* KOH + 0.17 *M* NaOH) solution at 300 °C for 24 h.

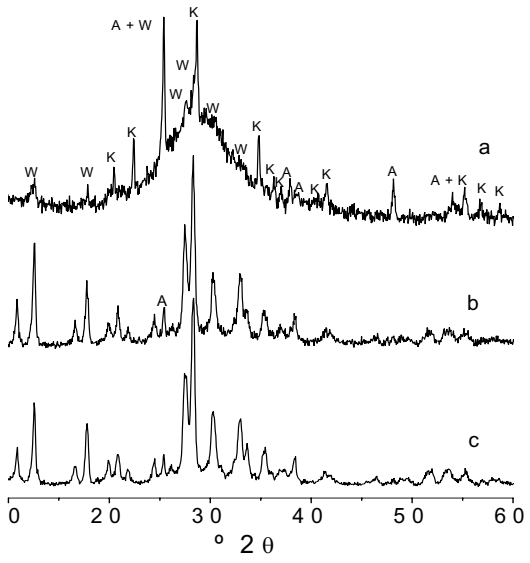

Figure 8. XRD pattern of the hydrothermal reaction product of kaolinite in 0.5 *M* KOH solution at 200 °C for (**a**) 24 h (W = zeolite W, K = kalsilite); (**b**) 48 h (zeolite W along with A = anatase); and (**c**) 120 h (zeolite W).

Kaolinite transforms into $P6_3$ kalsilite (a low-temperature form of $KAlSiO_4$) after hydrothermal treatment at 300 °C for 12 h in 0.5 *M* KOH solution. Longer reaction times increase the crystallinity of the structure, whereas shorter reaction times give rise to the metastable $KAlSiO_4$ polymorph with ABW zeolite-type unit cell. Lower temperatures are not sufficient to produce kalsilite, but zeolite W is obtained instead as the unique reaction product. Finally, pH of the aqueous solution in contact with kaolinite is an important parameter for the synthesis of kalsilite, which must be ≥13.70 if a temperature of 200 °C is used; otherwise, zeolite W is obtained.

Acknowledgments

M. Carmen Jiménez and Olga Montes are gratefully acknowledged for help with SEM and TEM, respectively. This work was supported by the European Union VI Framework Programme as an HRM Activity (contract no. MRTN-CT-2006-035957), DGICYT (project no. CTQ2007-63297), and Junta de Andalucía (Excellence Project P06-FQM-02179).

References cited

Andou, Y. and Kawahara, A. (1984) The refinement of the structure of synthetic kalsilite. Mineralogical Journal, 12, 153–161.

Barrer, R.M. and Baynham, J.W. (1956) The hydrothermal chemistry of silicates. Part VII. Synthetic potassium alumosilicates. Journal of the Chemical Society (Resumed), 2882–2891.

Barrer, R.M. and Mainwaring, D.E. (1972) Chemistry of soil minerals. Part XI. Hydrothermal transformations of metakaolinite in potassium hydroxide. Journal of the Chemical Society, Dalton Transactions, 1254–1259.

Barrer, R.M. and White, E.A.D. (1951) The hydrothermal chemistry of silicates. Part I. Synthetic lithium alumosilicates. Journal of the Chemical Society (Resumed), 1267–1278.

Barrer, R.M., Cole, J.F., and Sticher, H. (1968) Chemistry of soil minerals. Part V. Low temperature hydrothermal transformations of kaolinite. Journal of the Chemical Society A, 2475–2485.

Bieniok, A., Bornholdt, K., Brendel, U., and Baur, W.H. (1996) Synthesis and crystal structure of zeolite W, resembling the mineral merlinoite. Journal of Materials Chemistry, 6, 271–275.

Bogdanoviciene, I., Jankeviciute, A., Pinkas, J., Beganskiene, A., and Kareiva, A. (2007) Sol-gel synthesis and characterization of kalsilite-type alumosilicates. Materials Science, Kannaslitva, 13, 214–218.

Bogdanoviciene, I., Jankeviciute, A., Pinkas, J., Beganskiene, A., and Kareiva, A. (2008) Study of alumosilicate porcelains: Sol-gel preparation, characterization, and erosion evaluated by gravimetric method. Materials Research Bulletin, 43, 2998–3007.

Carpenter, M.A. and Cellai, D. (1996) Microstructures and high-temperature phase transitions in kalsilite. American Mineralogist, 81, 561–584.

Cellai, D., Carpenter, M.A., and Heaney, P.J. (1992) Phase transitions and microstructures in natural kaliophilite. European Journal of Mineralogy, 4, 1209–1220.

Cellai, D., Bonazzi, P., and Carpenter, M.A. (1997) Natural kalsilite, $KAlSiO_4$, with $P31c$ symmetry: Crystal structure and twinning. American Mineralogist, 82, 276–279.

Cheary, R.W. and Coelho, A. (1992) A fundamental parameters approach to X-ray line-profile fitting. Journal of Applied Crystallography, 25, 109–121.

Cook, L.P., Roth, R.S., Parker, H.S., and Negas, T. (1977) The system K_2O-Al_2O_3-SiO_2; Part 1, Phases on the $KAlSiO_4$–$KAlO_2$ join. American Mineralogist, 62, 1180–1190.

Dimitrijevic, R. and Dondur, V. (1995) Synthesis and characterization of $KAlSiO_4$ Polymorphs on the SiO_2-$KAlO_2$ join. II. The end-member of ANA-type zeolite framework. Journal of Solid State Chemistry, 115, 214–224.

Dollase, W.A. and Freeborn, W.P. (1977) The structure of $KAlSiO_4$ with $P6_3mc$ symmetry. American Mineralogist, 62, 336–340.

Dowty, E. (1987) Vibrational interactions of tetrahedra in silicates glasses and crystals: II. Calculations on melilites, pyroxenes, silica polymorphs and feldspars. Physics and Chemistry of Minerals, 14, 122–138.

Gregorkiewitz, M., Li, Y., White, T.J., Withers, R.L., and Sobrados, I. (2008) The structure of "orthorhombic" $KAlSiO_4$-O1: Evidence for Al-Si order from MAS NMR data combined with Rietveld refinement and electron microscopy. Canadian Mineralogist, 46, 1511–1526.

Hamilton, D.L. and Henderson, C.M.B. (1968) The preparation of silicate compositions by a gelling method. Mineralogical Magazine, 36, 832–838.

Heller-Kallai, L. and Lapides, I. (2003) Thermal reactions of kaolinite with potassium carbonate. Journal of Thermal Analysis and Calorimetry, 71, 689–698.

Henderson, C.M.B. and Taylor, D. (1988) The structural behavior of the nepheline family: (3) Thermal expansion of kalsilite. Mineralogical Magazine, 52, 708–711.

Hovis, G.L., Spearing, D.R., Stebbins, J.F., Roux, J., and Clare, A. (1992) X-ray powder diffraction and ^{23}Na, ^{27}Al and ^{29}Si MAS-NMR investigation of nepheline-kalsilite crystalline solutions. American Mineralogist, 77, 19–29.

Kawahara, A., Andou, Y., Marumo, F., and Okuno, M. (1987) The crystal structure of high temperature form of kalsilite ($KAlSiO_4$) at 950 °C. Mineralogical Journal, 13, 260–270.

Kimura, R., Wakabayashi, J., Elangovan, S.P., Ogura, M., and Okubo, T. (2008) Nepheline from K_2CO_3/Nanosized sodalite as a prospective candidate for diesel soot combustion. Journal of the American Chemical Society, 130, 12844–12845.

Kopp, O.C., Harris, L.A., and Clark, G.W. (1961) The hydrothermal conversion of muscovite to kalsilite and an iron-rich mica. American Mineralogist, 46, 719–727.

Kosanović, C., Subotić, B., Šmit, I., and Čižmek, A. (1997) Study of structural transformations in potassium-exchanged zeolite A induced by thermal and mechanochemical treatments. Journal of Materials Science, 32, 73–78.

Massiot, D., Fayon, F., Capron, M., King, I., Le Calvé, S., Alonso, B., Durand, J.O., Bujoli, B., Gan, Z., and Hoatson, G. (2002) Modeling one- and two-dimensional solid state NMR spectra. Magnetic Resonance in Chemistry, 40, 70–76.

Minor, D.B., Roth, R.S., Brower, W.S., and McDaniel, C.L. (1978) Alkali ion exchange reactions with $RbAlSiO_4$: A new metastable polymorph of $KAlSiO_4$. Materials Research Bulletin, 13, 575–581.

Norby, P. and Fjellvåg, H. (1992) Preparation, structural, and thermal properties of $MAlSiO_4$ (M = Li, Na, K, Rb, Cs, Tl, Ag) of ABW-type. Zeolites, 12, 898–908.

Norby, P., Christensen, A.N., and Krogh Andersen, I.G. (1986) Hydrothermal preparation of zeolite Li-A(BW), $LiAlSiO_4 \cdot H_2O$, and structure determination from powder diffraction data by direct methods. Acta Chemica Scandinavica A, 40, 500–506.

Perrotta, A.J. and Smith, J.V. (1965) The crystal structure of kalsilite, $KAlSiO_4$. Mineralogical Magazine, 35, 588–595.

Sahama, Th.G. (1965) Infrared absorption of nepheline. Comptes Rendus de la Société Geologique de Finlande, 37, 107–117.

Smith, J.V. and Tuttle, O.F. (1957) The nepheline-kalsilite system; Part I, X-ray data for the crystalline phases. American Journal of Science, 255, 282–305.

Sobrados, I. and Gregorkiewitz, M. (1993) Ion exchange between tectosilicates with the nepheline-kalsilite framework and molten MNO_3 or MO (M = Li, Na, K, Ag). Physics and Chemistry of Minerals, 20, 433–441.

Stebbins, J.F., Murdoch, J.B., Carmichel, I.S.E., and Pines, A. (1986) Defects and short-range order in nepheline group minerals: a silicon-29 nuclear magnetic resonance study. Physics and Chemistry of Minerals, 13, 371–381.

Zhang, Y., Ming, L., Chen, D., and Wu, J. (2007) Leucite crystallization kinetics with kalsilite as a transition phase. Materials Letters, 61, 2978– 2981.

Manuscript received May 7, 2009
Manuscript accepted July 24, 2009
Manuscript handled by Warren Huff